THE ASTROPHYSICAL JOURNAL, 404:38–50, 1993 February 10

VELOCITY DISPERSIONS IN GALAXY CLUSTERS

M. GIRARDI,[1] A. BIVIANO,[1,2,3] G. GIURICIN,[1,2] F. MARDIROSSIAN,[1,2] AND M. MEZZETTI[1,2]

Received 1992 June 2; accepted 1992 August 5

ABSTRACT

We analyze the velocity dispersions of 79 galaxy clusters having at least 30 galaxies with available redshifts. We show that different estimates of velocity dispersion give similar results on cluster samples of at least ∼20 galaxies each. However, only robust estimates of velocity dispersion seem to be efficient on cluster samples with ∼10 galaxies each. A significant correlation is found to exist between the velocity dispersion and the cluster richness. We provide the distribution function of cluster velocity dispersions, normalized to the complete sample by Abell, Corwin, & Olowin (1989). Available theoretical models are compared with this distribution function.

Subject headings: galaxies: clustering — galaxies: distances and redshifts

1. INTRODUCTION

The distribution functions of observational cluster quantities, such as velocity dispersions, radii, masses, luminosities, and X-ray temperatures, can provide strong constraints both on cosmological scenarios and on the internal dynamics of these systems. Theoretical as well as observational estimates of these distribution functions are presently being debated.

The theoretical mass distribution expected for groups and clusters in the hierarchical clustering scenario has been derived by several authors (see, e.g., Press & Schechter 1974; Cavaliere, Colafrancesco, & Scaramella 1991). Saslaw and collaborators (see, e.g., Inagaki, Itoh, & Saslaw 1992 and references therein) derived the galaxy distribution functions in space and velocity, in the context of their thermodynamic theory. Peebles, Daly, & Juszkiewicz (1989) showed that no values of the b biasing parameter and the clustering correlation length are consistent with all the available observational constraints. Henry & Arnaud (1991) constrained the mass fluctuation spectrum using the distribution function of cluster X-ray temperatures, and obtained a value of $b = 1.7$, but they found a disagreement with the index of the fluctuation power spectrum predicted by CDM models on the cluster scale. Lilje (1992) showed that the distribution functions for mass and X-ray temperature (or velocity dispersion) of rich clusters provide important diagnostics for cosmological models. He found a better agreement of the observations with an antibiased low-density CDM model than with the standard CDM model.

In this paper we specifically address the distribution function of velocity dispersions for galaxy clusters. One can find several cluster-monographic analyses of velocity dispersions in the literature (see, e.g., Kent & Gunn 1982; Kent & Sargent 1983; Binggeli, Tammann, & Sandage 1987; Sharples, Ellis, & Gray 1988); however, very large redshift samples have only recently become available (see, e.g., Colless & Hewett 1987; Dressler & Schectman 1988a; Zabludoff, Huchra, & Geller 1990, hereafter ZHG; Teague, Carter, & Gray 1990; Beers et al. 1991; see also Struble & Rood 1991). These samples have allowed detailed study of the distribution function of cluster velocity dispersions.

Evrard (1989) examined the distribution of cluster velocity dispersions in the context of a CDM–dominated universe, and he found that different values of b are needed for the high-redshift cluster population and the low-redshift one. Frenk et al. (1990, hereafter FWED) calculated the distributions of velocity dispersion, gas temperature, and mass-to-light ratios for Abell clusters in the CDM model. FWED compared their theoretical distributions with observations, yielding a value of b in the range 2–3 (after taking into account the projection effects). From a sample of 69 nearby Abell clusters, with at least 10 measured redshifts within 1.5 h_{100}^{-1} Mpc of the cluster center, ZHG obtained a velocity dispersion distribution consistent with the CDM models by FWED, with $b \sim 1.6$–2.0.

Recently, Davis et al. (1992, hereafter DEFW) have called into question the whole CDM scenario, and even the very latest results by *COBE* (Bennett et al. 1992; Smoot et al. 1992) do not provide support for the CDM. The *COBE* results may be in agreement with decaying HDM models (see Scott, Rees, & Sciama 1991). On the other hand, HDM models have not been detailed so deeply as to allow a direct comparison between observational and theoretical cluster distribution functions (see, e.g., Lilje & Lahav 1991, and Trimble 1987 with references therein).

In this framework, we deemed it interesting to obtain a velocity dispersion distribution from the best sampled clusters of galaxies available in the literature. We collected 79 clusters with at least 30 measured galaxy redshifts. Our choice of a minimum of 30 galaxy redshifts per cluster is a compromise between obtaining a reliable estimate of the kinematics of each cluster and producing a sufficiently extended and detailed distribution function.

A fair estimate of a cluster velocity dispersion in a cluster faces some problems, i.e., the presence of foreground and background interlopers, the unknown underlying velocity distribution of galaxies, the presence of substructures, and the limited amount of data available. In the literature one can find several estimates of the scale ("dispersion") of velocity distribution in clusters. The one most extensively used is that by Yahil & Vidal (1977. hereafter YV), the so-called 3 σ–clipping technique. Beers, Flynn, & Gebhardt (1990, hereafter BFG) approached the problem in a well-defined statistical way, suggesting the use of robust estimators, such as the "biweight" and the "gapper." A simplified form of the "gapping" procedure was previously introduced by ZHG.

[1] Scuola Internazionale Superiore di Studi Avanzati, Strada Costiera 11, 34014-Trieste, Italy.
[2] Dipartimento di Astronomia, Università degli Studi di Trieste.
[3] Also International Centre for Theoretical Physics, Trieste.

In order to obtain the distribution function of cluster velocity dispersions, it is necessary to face these problems in a homogeneous way for a large enough sample of clusters.

In § 2 we describe the data sample we used. In § 3 we compare several different estimates of cluster velocity dispersion, and we check the Gaussianity of the parent distributions of velocities. Then we test the sensitivity of the velocity dispersion estimate on possible observational biases, i.e., different limiting radii, incompleteness in magnitude, and the small number of redshifts. We also address the problem of substructure. The velocity dispersions are then examined in relation to other optical properties of clusters. Finally, we compare the distribution function of our cluster velocity dispersions with CDM theoretical predictions. In § 4 we provide the relevant discussion and our conclusions.

2. THE DATA AND SAMPLE

We have collected data for clusters having at least 30 galaxies with measured redshifts (and positions) in the literature. Clusters with mean redshift $\bar{z} > 0.15$ have not been considered, so as not to bother with possible evolutionary effects (see, e.g., Newberry, Kirshner, & Boronson, 1988). Our final sample contains a total of $\sim$7000 galaxies belonging to 79 clusters. In order to achieve a sufficiently homogeneous sample, all the galaxy redshifts in each cluster have usually been taken from one reference source only, or from different sources, when these were compatible. All the velocities have been transformed into the local standard of rest, according to Chapman, Geller, & Huchra (1987).

We have collected magnitudes for a total of $\sim$5500 galaxies in 66 clusters of our sample; 32 of these clusters are also complete (or nearly complete) in magnitude. These magnitudes have been corrected for K-dimming effect and absorption by our own Galaxy. The K-dimming corrections for the R, V, and B bands are from Sandage (1973); the corrections for the r, g magnitude system are from Schneider, Gunn, & Hoessel (1983), and for the J system from Phillips, Fong, & Shanks (1981). The absorptions by our Galaxy are from Burstein & Heiles (1982); the relations between absorptions in different bands are from Sandage (1973) and Schneider et al. (1983). We have transformed all these magnitudes into the visual photometric band, using the formulae given by Oemler (1974), Schweizer (1976), Thuan & Gunn (1976), de Vaucouleurs (1977), Kirshner, Oemler, & Schechter (1978), Geller et al. (1984), Shanks et al. (1984), Postman, Huchra, & Geller (1986), and Colless (1989).

The galaxy morphological types are available for most galaxies in 40 clusters of our sample.

In order to reject the possible noncluster members from our samples, we have adopted the following procedure. First, we have rejected galaxies beyond 3 h_{100}^{-1} Mpc from the cluster center. The cluster luminosity distance ($H_0 = 100$ km s^{-1} Mpc, $q_0 = \frac{1}{2}$) is deduced from the mean redshift, computed via the biweight location estimator (see BFG). The cluster centers come from Abell, Corwin, & Olowin (1989, hereafter ACO), when available, otherwise, from the sources of the data. Then, following Beers et al. (1991), we have eliminated galaxies with velocities differing by more than 4000 km s^{-1} from the cluster velocity center, computed via the biweight location estimator (see BFG).

At this step, we have computed the errors on cluster velocity dispersions via a bootstrap technique (see, e.g., Efron & Tibshirani 1986). This method consists in computing the quantity of interest (velocity dispersion in the present case) of a statistically large number of random data sets extracted (even with repetition) from the original velocities. Our results are based on 10,000 resamplings. The bootstrap method does not rely on any a priori assumption of the underlying data distribution; therefore, it is more robust than traditional error estimates, since the cluster velocity distribution is unknown (see, e.g., BFG).

This analysis has shown that some cluster velocity dispersions were affected by large errors. In particular, five clusters had $\delta_{68} > 250$ km s^{-1}, where we denote by δ_{68} the bootstrap error on the velocity dispersion at the 68% confidence level. Moreover, some very well sampled clusters still showed evidence of contamination by obvious interlopers (see, e.g., in Fig. 1, the obvious backgound group in the Virgo sample).

We have therefore performed a further rejection of galaxies, based on the weighted gaps in the velocity distributions (see BFG). A weighted gap in the space of the ordered velocities, $v_1 \leq v_2 \leq \cdots \leq v_n$, is defined as the difference between two contiguous velocities, weighted according to their positions in the ordered distribution: the closer to the center of the distribution is the gap, the higher is its weight. Specifically, we have rejected galaxies separated in velocity space from the main cluster body by a weighted gap ≥ 4. This procedure is sufficient to clean the velocity space of clearly contaminated clusters (like Virgo, see Fig. 1), although it has little effect on most of our clusters. After this rejection, only one cluster still has $\delta_{68} > 250$ km s^{-1} (ACO 2092).

On the remaining galaxies, we have computed the cluster centers, using the biweight location estimator for position (right ascension and declination, separately). From now on, we shall consider only those clusters (79) with at least 20 galaxies inside 1.5 h_{100}^{-1} Mpc (one Abell radius). Our final cluster sample is described in Table 1; in column (1) we list the cluster names; columns (2) and (3) contain the number of collected galaxies with available redshift in each cluster region and the number of member galaxies inside 1.5 h_{100}^{-1} Mpc, respectively; columns (4)–(6) list the richness class, R, Abell count, C, and Bautz-Morgan type, BM, respectively, from ACO or from the sources of the velocity and/or magnitude data; in column (7) we list the Rood-Sastry type, RS, mainly from Struble & Rood (1987); column (8) contains the number counts by Bahcall (1977, 1981), N; in column (9) "mc" (or "$\sim$mc") labels those clusters which are complete (or nearly complete), to some limiting magnitude, according to the references in column (11); the relevant references for the galaxy redshifts, magnitudes and morphological types are listed in columns (10)–(12), respectively.

3. ANALYSIS AND RESULTS

3.1. *Estimates of Velocity Dispersion*

We have compared three different methods used to estimate the velocity dispersion (or, more precisely, the scale of the velocity distribution): (1) the classical 3 σ–clipping estimate (YV), $\sigma_{\rm YV}$; (2) the simplified gapping estimate by ZHG, $\sigma_{\rm ZHG}$; (3) a "robust" estimate, $\sigma_{\rm rob}$, which is the "gapper" scale estimator when the number of galaxies in the sample is <15, and the "biweight" estimator otherwise (see BFG; see also Teague et al. 1990; Beers et al. 1991; Gebhardt & Beers 1991; Biviano et al. 1992). We have corrected the velocity dispersions for the velocity errors as in Danese, De Zotti, & di Tullio (1980); in our samples, this correction was always very small ($\sim$few km s^{-1}).

The procedure of YV eliminates all the galaxies with velocities deviating more than 3 σ from the mean velocity, in an

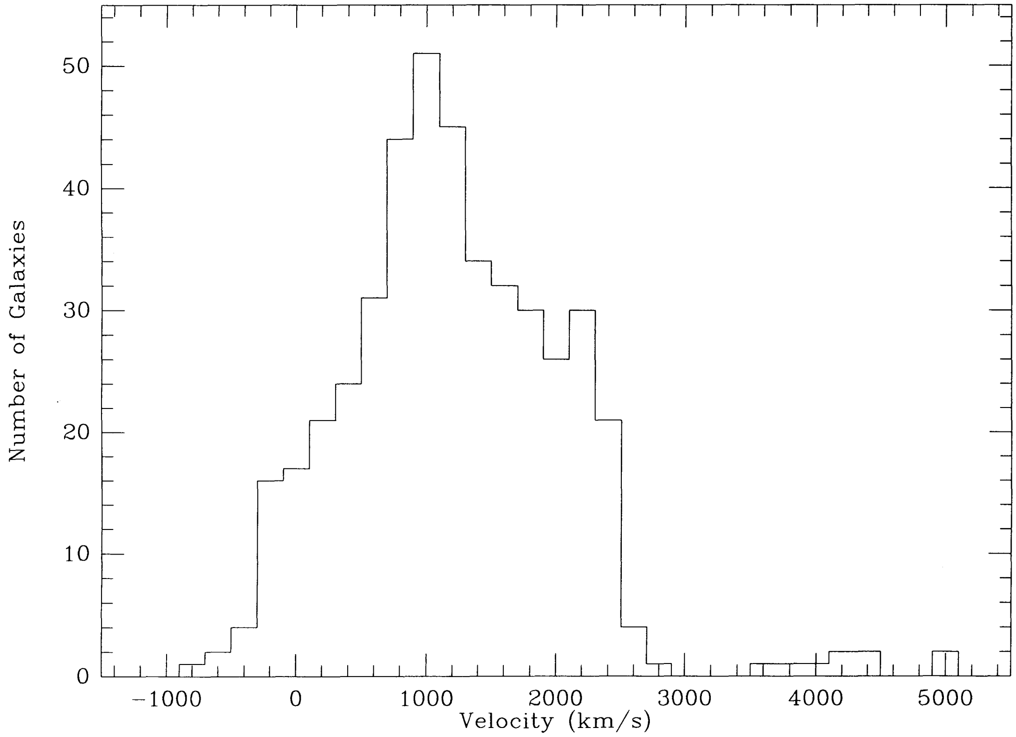

FIG. 1.—Velocity histogram for the Virgo Cluster. Notice the obvious background group at $\sim$4000 km s^{-1}.

iterative fashion. ZHG remove any galaxy separated in the velocity space from the previous one by more than the value of the velocity dispersion. After eliminating these galaxies, both YV and ZHG compute the standard velocity dispersion. The gapper estimator is based on the weighted gaps in the velocity space (see § 2), while the biweight estimator is obtained via a specific function of the deviations of the velocities from their median value, removing very isolated velocities. However, see YV, ZHG, and BFG for a more detailed description of these estimators.

We have considered different regions in each cluster, by selecting galaxies within different limiting distances from each cluster center, $d \leq 0.125$, 0.25, 0.50, 0.75, 1.00, 1.50, 2.00, 3.00 h_{100}^{-1} Mpc. Regions containing fewer than six galaxies have not been considered in our analyses. When not stated otherwise, we will hereafter quote results concerning the region inside 1.5 h_{100}^{-1} Mpc.

We have applied the Kruskall-Wallis test (see, e.g., Ledermann 1982) to compare σ_{YV}, σ_{ZHG}, and σ_{rob} for our cluster samples. We have not found any significant difference. In Figure 2 we plot the cumulative distributions of σ_{rob}, σ_{YV}, and σ_{ZHG} at 1.5 h_{100}^{-1} Mpc from each cluster center. Only in the region inside 0.25 h_{100}^{-1} Mpc have we detected a very marginal difference at the significance level (s.l. in tyhe following) of 93%. The most discordant distributions are those of σ_{ZHG} and σ_{rob}, which differ at a s.l. of 98.6%, according to a Kolmogorov-Smirnov test (hereafter KS test; see, e.g., Ledermann 1982); the Mann-Whitney U-test and the Rank-Sum T-test (hereafter U-test and T-test, respectively; see, e.g., Kendall & Stuart 1977; Hoel 1971) give similar results. However, we must stress that ZHG did not use their dispersion estimate in such small regions.

The mean values of the velocity dispersion of our cluster sample, inside 1.5 h_{100}^{-1} Mpc, are $\langle\sigma_{YV}\rangle = 754 \pm 31$, $\langle\sigma_{ZHG}\rangle = 761 \pm 28$, $\langle\sigma_{rob}\rangle = 786 \pm 29$ km s^{-1}. Therefore, the observed velocity dispersions for our cluster sample do not seem to depend on the estimator adopted.

3.2. *Testing the Gaussianity*

The results of § 3.1 suggest that the distributions of galaxy velocities in our clusters are nearly Gaussian. In fact, YV's technique is devised for Gaussian distributions, while the robust estimators are much less sensitive to the assumed nature of the population from which the data are drawn. We have considered four estimators of Gaussianity: the kurtosis, K; the skewness, S; the scaled tail index, STI (see, e.g., Beers et al. 1991); the probability associated to the W-test, $P(W)$ (Shapiro & Wilk 1965). The reference values for a Gaussian distribution are $K = 3$, $S = 0$, STI $= 1$, and $P(W) = 1$. We have obtained the estimates of K, S, STI, and $P(W)$, for each of our clusters, separately.

In order to measure the deviations from Gaussianity, we have computed the ratios $|(K-3)/\delta_K|$, and $|S/\delta_S|$, where δ_K and δ_S denote the errors on K and S, respectively, These ratios happen to be correlated to one another, and are anticorrelated with $P(W)$ (s.l. > 99% in all correlations), as expected if they are good and coherent estimators of the shape of the distribution. Moreover, these three quantities are strongly correlated with $|\sigma_{rob} - \sigma_{YV}|$ and $|\sigma_{rob} - \sigma_{ZHG}|$; i.e., the more the distributions deviate from Gaussianity, the more the robust and classical dispersion estimates differ.

The null hypothesis of a Gaussian parent distribution is rejected (at a 3 standard deviations s.l.) by at least one of the above-mentioned tests, for 14 clusters only. The non-Gaussian clusters are reduced to three, when only galaxies inside 0.5 h_{100}^{-1} Mpc are considered. The mean values of the Gaussian estimators in our cluster sample are $K = 3.6 \pm 0.2$, $S = 0.04 \pm 0.08$, STI $= 1.10 \pm 0.03$, and $P(W) = 0.31 \pm 0.04$. These values

TABLE 1

THE DATA SAMPLE

NAME (1)	N_{tot} (2)	$N_{1.5}$ (3)	R (4)	C (5)	BM (6)	RS (7)	N (8)	COMPLETENESS (9)	REFERENCES Velocity (10)	Magnitude (11)	Type (12)
ACO 151	58	28	1	72	II	cD	-		[1]	[2]	[2]
ACO 194	268	68	0	37	II	L	15	~mc	[3]	[3]	[4]
ACO 262	88	48	0	40	III	C	14		[5,6,7]	[8]	[5,6,7]
ACO 426 (Perseus)	200	151	2	88	II-III	L	33	~mc	[9]	[8,9]	[9]
ACO 458	45	32	2	114	I-II	cD	-		[10]	[11]	
ACO 496	34	34	1	50	I	cD	14		[12]	[13]	[13]
ACO 539	289	77	1	50	III	F	-	~mc	[14]	[8,15]	[14]
ACO 548	134	117	1	79	III	F	-	mc	[13]	[13]	[13]
ACO 569	41	27	0	36	II	B	-		[16]		
ACO 576	51	48	1	61	III	I	25		[17]	[18]	[18]
ACO 754	89	68	2	92	I-II	cD	30	mc	[13]	[13]	[13]
ACO 957	39	32	1	55	I-II	L	-		[16]	[2]	[2]
ACO 999	45	24	0	33	II-III	L	-	mc	[19]	[20]	[20]
ACO 1016	44	22	0	37	-	L	-	~mc	[19]	[20]	[20]
ACO 1060 (Hydra)	177	134	1	50	III	C	13	mc	[21,22]	[21,22]	[21,22]
ACO 1142	66	42	0	35	II-III	C	-	~mc	[23]	[13]	[13]
ACO 1146	84	55	4	222	-	cD	28		[24]		
ACO 1185	77	29	1	52	II	C	-		[16]		
ACO 1367	94	73	2	117	II-III	F	18		[25,26,27,28]	[8]	[25,26,27,28]
ACO 1631	90	58	0	34	I	C	-	mc	[13]	[13]	[13]
ACO 1644	102	77	1	68	II	cD	-	mc	[13]	[13]	[13]
ACO 1651	31	29	1	70	I-II	cD	-		[29]		
ACO 1656 (Coma)	414	226	2	106	II	B	28	mc	[30]	[30]	[30]
ACO 1736a	40	34	-	-	-	-	-	mc	[13]	[13]	[13]
ACO 1736b	64	54	-	-	-	-	-	mc	[13]	[13]	[13]
ACO 1750	55	47	0	40	II-III	F	-		[16]		
ACO 1795	45	40	2	115	I	cD	27		[31]		
ACO 1983	100	67	1	51	III	F	-	mc	[13]	[13]	[13]
ACO 1991	71	25	1	60	I	F	-		[16]	[2]	[2]
ACO 2052	43	41	0	41	I-II	cD	-		[32]	[8]	
ACO 2063	73	37	1	63	II	cD	-		[16]	[2]	[2]
ACO 2065	31	25	2	109	III	C	50		[33]	[33]	
ACO 2079	32	26	1	57	II-III	cD	-	mc	[34]	[34]	
ACO 2092	30	20	1	55	II-III	I	-		[34]	[34]	
ACO 2147/2152	45	38	-	-	III	-	-		[35]	[8]	[35]
ACO 2151 (Hercules)	105	96	2	87	III	F	18	mc	[13]	[13]	[13]
ACO 2197	45	41	1	73	III	L	6		[36]	[8]	
ACO 2199	71	60	2	88	I	cD	19		[36]	[8]	[37,38]
ACO 2256	89	86	2	88	II	B	32	mc	[39]	[39]	
ACO 2440	30	24	0	32	II	L	24		[16]		
ACO 2538	45	42	1	72	II-III	C	-		[10]	[11]	
ACO 2554	41	28	3	159	II	L	-		[10]	[11]	
ACO 2589	33	33	0	40	I	cD	20		[16]		
AC0 2593	37	36	0	42	II	F	-		[16]		
ACO 2670	303	196	3	142	I-II	cD	-	mc	[40]	[40]	[40]
ACO 2717	45	33	1	52	I-II	-	-		[10]	[11]	
ACO 2721	88	61	3	192	II	L	-		[24]	[11]	
ACO 3126	45	38	1	75	III	-	-		[10]	[11]	
ACO 3128	45	44	3	140	I-II	-	-		[10]	[11]	
ACO 3158	37	34	2	85	I-II	L	-		[41,42]	[41]	[42]
ACO 3225	44	41	0	37	II	-	-		[10]	[11]	
ACO 3266	172	130	2	91	I-II	cD	-		[24]		
ACO 3334	41	32	2	82	I-II	-	-		[10]	[11]	
ACO 3360	40	37	2	85	III	-	-		[10]	[11]	
ACO 3376	84	67	0	42	I	-	-	mc	[13]	[13]	[13]
ACO 3381	64	29	1	69	I	-	-	mc	[13]	[13]	[13]
ACO 3389	39	39	0	35	II-III	C	-		[24]	[13]	[13]
ACO 3391	81	66	0	40	I	cD	-		[24]		
ACO 3395	203	143	1	54	II	C	19		[24]		

TABLE 1—*Continued*

Name (1)	N_{tot} (2)	$N_{1.5}$ (3)	R (4)	C (5)	BM (6)	RS (7)	N (8)	Completeness (9)	References: Velocity (10)	References: Magnitude (11)	References: Type (12)
ACO 3526 (Centaurus)	301	164	0	33	I-II	I	15		[43,44]	[43,44]	[43,44]
ACO 3532 (Klemola 22)	44	43	0	36	II-III	-	-		[45]	[45]	
ACO 3558 (Shapley 8)	123	113	4	226	I	cD	-	mc	[24,46]	[46]	
ACO 3574	42	38	0	31	I	-	-	~mc	[47]	[47]	[47]
ACO 3667	48	45	2	85	I-II	L	-		[48]	[48]	
ACO 3705	45	40	2	100	III	-	-		[10]	[11]	
ACO 3716	106	77	1	66	I-II	-	-	mc	[13]	[13]	[13]
ACO 4067	41	29	1	72	III	F	-		[24]		
ACO S301	30	29	0	5	I	-	-	mc	[13]	[13]	[13]
ACO S373 (Fornax)	57	56	0	-18	I	-	-	~mc	[44]	[44]	[44]
ACO S463	100	79	0	26	I-II	-	-	mc	[13]	[13]	[13]
ACO S753	43	34	0	18	I	-	-	~mc	[47]	[47]	[47]
ACO S805	50	42	0	8	I	-	-		[49]	[49]	[49]
AWM 1	56	25	0	-	II-III	-	-	mc	[50]	[50]	[50]
AWM 7	33	33	0	-	I	-	17	mc	[50]	[50]	[50]
Colless 67	45	28	1	-	I-II	-	-		[10]	[11]	
Dressler 0003-50	55	34	-	-	-	-	-	mc	[13]	[13]	[13]
MKW 4	86	43	0	-	I	-	-		[50,51]	[50,51]	[50,51]
Pegasus I	78	36	0	-	II	-	-		[52,53,54]	[52,53,54]	[52,53,54]
Virgo	572	413	1	-	III	I	11	mc	[55]	[55]	[55]

Explanation of Columns.—Col. (1): Cluster name; Col. (2): Total number of galaxies with available redshift in the original sample; Col. (3): Number of member galaxies within 1.5 h_{100}^{-1} Mpc from the cluster center; Col. (4): Richness class, R; Col. (5): Abell number counts, C; Col. (6): Bautz-Morgan type, BM; Col. (7): Rood-Sastry type, RS; Col. (8): Bahcall number counts, N; Col. (9): "mc" (or " ~mc") labels those clusters which are complete (or nearly complete) to some limiting magnitude.

References.—(1) Proust et al. 1992; (2) Dressler 1980; (3) Chapman, Geller, & Huchra 1988; (4) Chincarini & Rood 1977; (5) Giovanelli, Haynes, & Chincarini 1982; (6) Gregory, Thompson, & Tifft 1981; (7) Moss & Dickens 1977; (8) Zwicky et al. 1961–1968; (9) Kent & Sargent 1983; (10) Colless & Hewett 1987; (11) Colless 1989; (12) Mazure et al. 1986; (13) Dressler & Shectman 1988b; (14) Ostriker et al. 1988; (15) Nilson 1973; (16) Beers et al. 1991; (17) Hintzen et al. 1982; (18) Fanti et al. 1982; (19) Chapman, Geller, & Huchra 1987; (20) Adams, Strom, & Strom 1980; (21) Richter 1987; (22) Richter 1989; (23) Geller et al. 1984; (24) Teague, Carter, & Gray 1990; (25) Gavazzi 1987; (26) Gregory & Thompson 1978; (27) Tifft 1978; (28) Dickens & Moss 1976; (29) Zabludoff, Huchra, & Geller 1990; (30) Kent & Gunn 1982; (31) Hill et al. 1988; (32) Quintana et al. 1985; (33) Postman, Geller, & Huchra 1988; (34) Postman, Huchra, & Geller 1986; (35) Tarenghi et al. 1979; (36) Gregory & Thompson 1984; (37) Tifft 1974; (38) Butcher & Oemler 1985; (39) Fabricant, Kent, & Kurtz 1989; (40) Sharples, Ellis, & Gray 1988; (41) Chincarini, Tarenghi, & Bettis 1981; (42) Lucey et al. 1983; (43) Dickens, Currie, & Lucey 1986; (44) Lauberts & Valentijn 1989; (45) Cristiani et al. 1987; (46) Metcalfe, Godwin, & Spenser 1987; (47) Willmer et al. 1991; (48) Proust et al. 1988; (49) Bell & Whitmore 1989; (50) Beers et al. 1984; (51) Malumuth & Kriss 1986; (52) Richter & Huchtmeier 1982; (53) Bothun et al. 1985; (54) Chincarini & Rood 1976; (55) Binggeli, Sandage, & Tammann 1985.

show that there is no systematics in the deviations from Gaussianity of the velocity distributions of our clusters.

In Table 2 we list the following quantities: column (1), cluster name; column (2), σ_{rob}, with its associated bootstrap errors, at the 68% confidence level; columns (3) and (4), σ_{YV}, and σ_{ZHG}, respectively; columns (5), (6), (7), and (8), K, S, STI, and $P(W)$, respectively; columns (9) and (10), the ratios $|(K-3)/\delta_K|$, and $|S/\delta_S|$. All quantities are computed inside 1.5 h_{100}^{-1} Mpc.

3.3. *Efficiency of the Velocity Dispersion Estimates*

In order to check the statistical efficiency of the velocity dispersion estimates, we have artificially undersampled the velocity field in two ways: (1) we have randomly selected limited numbers of galaxies (10 and 15) from each cluster sample; (2) we have considered only cluster members more luminous than m_{10} (i.e., the magnitude of the tenth brightest galaxy in each cluster sample). In order to mimic the observations, the subsamples have been selected from the original samples, before cleaning them from the obvious interlopers (see § 2). On these subsamples we have then applied the procedure for the identification of " true " members.

A random sampling of galaxies in a cluster field may model observational selections (see, e.g., Colless & Hewett 1987). We have compared the distribution of the velocity dispersions computed on all galaxies, with those obtained with 10 and 15 galaxies randomly selected. In the case of both 10 and 15 objects, the velocity dispersions are obtained as the average of 1000 random samplings. According to the KS, U, and T tests, there is no significant difference when using σ_{rob}. The σ_{ZHG} distribution is partially different both with 10 and with 15 objects sampled (s.l. ~ 95%), while the σ_{YV} distribution is partially different only with 10 objects sampled.

The σ_{rob} distribution, as computed on the galaxies brighter than m_{10}, does not significantly differ from the distribution of σ_{rob}, as computed on all the galaxies (66 clusters with available magnitudes are considered here). On the contrary, the distributions of both σ_{YV} and σ_{ZHG} for the galaxies brighter than m_{10} are significantly different (>99% and >99.99% s.l., respectively), from the corresponding distributions for the total

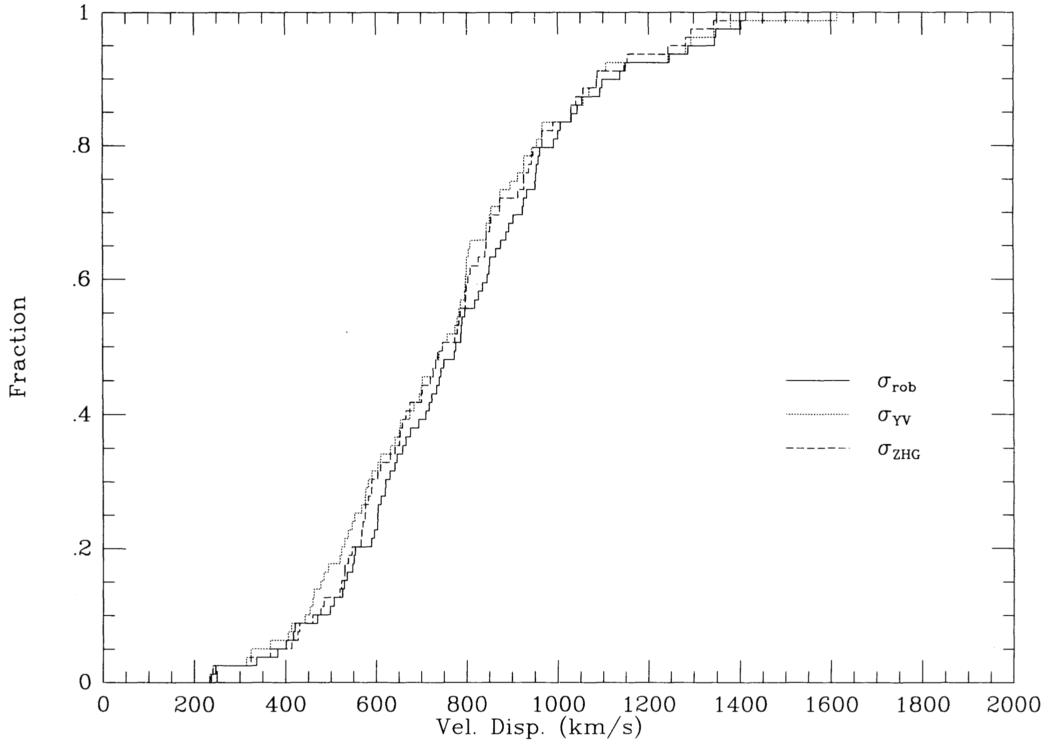

FIG. 2.—Cumulative distributions of σ_{rob} (*solid line*), σ_{YV} (*dotted line*), and σ_{ZHG} (*dashed line*), at 1.5 h_{100}^{-1} Mpc from each cluster center. The three distributions are not significantly different.

samples. As detailed in the discussion (§ 4), these differences may be due to the poor efficiency of σ_{YV} and σ_{ZHG}, and to the effect of luminosity segregation.

In Figure 3 we plot the cumulative distributions of σ_{rob} (Fig. 3*a*) and σ_{ZHG} (Fig. 3*b*) for the subsample of the galaxies brighter than m_{10} and for the total sample, respectively. The same test, applied to our subsample of 32 magnitude complete (or nearly complete) clusters—see Table 1, column (9)—has given similar results.

The average difference between the velocity dispersions, as computed on the total sample and on a subsample of 10 galaxies, has an absolute value of $\simeq 200$ km s^{-1}, for any estimator. However, σ_{YV} and σ_{ZHG} seem to systematically underestimate the velocity dispersion, when they are computed on 10 galaxies only, while σ_{rob} does not show any systematic trend.

Thus, in view of results of §§ 3.1 and 3.2, and according to the results obtained by BFG, we hereafter prefer to rely on the robust estimator of the velocity dispersion.

3.4. *Subclustering and Velocity Dispersion*

It is clear that the presence of substructures can invalidate the significance of the measurement of cluster velocity dispersions. So, we have investigated the implication of possible subclustering in our data sample. We have adopted the procedure of Dressler & Shectman (1988b), using the robust location and scale estimators in place of the classical mean and dispersion. We have performed 1000 simulations in order to assess the probability of any substructures detected. This procedure gives the probability of subclustering for each cluster, without detailing the substructures. However, this method appears to be the most suitable for our data sample, since it does not require the knowledge of hundreds of cluster galaxy redshifts and positions.

We have compared the distribution of σ_{rob} for all clusters in our sample, with the corresponding distribution for the 50 clusters without significant evidence for substructure (i.e., at a s.l. < 90%). These distributions are not different according to the KS, *U*, and *T* tests. Most of the clusters with evidence for subclustering belong to $R = 0$, 1 classes; the same tests, applied to these clusters only, confirmed the previous results.

Our estimate of σ_{rob} does not seem to be seriously affected by the presence of substructures in the clusters of our sample. This result may indicate that subclustering does not grossly modify the dispersion estimates in our cluster sample. However, the average number of cluster members in our sample is not high enough to allow an extensive use of more sophisticated analyses of subclustering (see, e.g., Fitchett & Merritt 1988; Escalera & Mazure 1992). Moreover, the definition itself of subclustering is still under debate (see, e.g., West & Bothun 1990 and references therein). For all these reasons, we wish to consider the result of this section as preliminary.

3.5. *Increasing Apertures and Velocity Dispersion*

We have examined the distributions of σ_{rob} computed on the galaxies inside circles of increasing radii, from 0.125 to 3.0 h_{100}^{-1} Mpc; according to the KW test, these distributions are drawn from the same parent distribution at a s.l. > 99.9%. However, our clusters are not always sampled in all these regions (e.g., the clusters by Colless & Hewett 1987 are sampled inside 1 h_{100}^{-1} Mpc from the center), and only 46 of our clusters do contain galaxies as far as 1.5 h_{100}^{-1} Mpc from the center. On this subsample of 46 clusters, we have repeated the above analysis,

TABLE 2

VELOCITY DISPERSIONS AND GAUSSIANITY

Name (1)	σ_{rob} (2)	σ_{YV} (3)	σ_{ZHG} (4)	K (5)	S (6)	STI (7)	$P(W)$ (8)	$\|K-3\|/\delta_K$ (9)	$\|S\|/\delta_S$ (10)
ACO 151	603^{+95}_{-63}	590	590	2.63	0.25	0.96	0.72	0.43	0.56
ACO 194	421^{+53}_{-43}	405	431	15.67	-2.48	1.15	0.00	22.07	8.52
ACO 262	498^{+63}_{-55}	459	459	3.53	-0.20	1.03	0.98	0.78	0.59
ACO 426 (Perseus)	1288^{+90}_{-77}	1282	1282	2.99	0.28	1.03	0.30	0.02	1.39
ACO 458	893^{+213}_{-95}	795	937	4.08	-0.96	0.88	0.10	1.34	2.33
ACO 496	645^{+81}_{-77}	631	631	2.65	-0.27	1.00	0.73	0.45	0.68
ACO 539	787^{+107}_{-77}	739	840	4.00	-0.59	1.31	0.01	1.85	2.15
ACO 548	887^{+47}_{-39}	854	854	2.12	0.10	0.90	0.01	1.99	0.42
ACO 569	401^{+103}_{-67}	314	427	3.68	-1.03	1.06	0.04	0.78	2.30
ACO 576	1001^{+119}_{-96}	913	913	3.06	0.28	1.20	0.84	0.09	0.81
ACO 754	743^{+97}_{-76}	695	736	4.81	-0.48	1.20	0.56	3.16	1.65
ACO 957	952^{+201}_{-111}	851	851	4.20	-0.41	0.84	0.15	1.49	0.99
ACO 999	417^{+175}_{-88}	413	413	5.56	-1.60	1.52	0.00	2.79	3.39
ACO 1016	247^{+44}_{-33}	241	241	2.61	0.02	1.08	0.92	0.41	0.04
ACO 1060 (Hydra)	630^{+37}_{-33}	609	609	2.51	-0.08	1.05	0.18	1.17	0.39
ACO 1142	610^{+157}_{-122}	538	538	4.82	-0.25	1.26	0.04	2.54	0.69
ACO 1146	1137^{+155}_{-107}	1069	1154	3.43	0.11	1.21	1.00	0.68	0.34
ACO 1185	790^{+173}_{-91}	799	720	3.37	0.18	0.78	0.82	0.43	0.41
ACO 1367	835^{+94}_{-76}	798	798	4.39	-0.55	1.25	0.24	2.50	1.97
ACO 1631	694^{+70}_{-53}	674	674	2.51	0.07	1.00	0.76	0.79	0.24
ACO 1644	932^{+110}_{-76}	943	943	3.26	0.50	1.02	0.24	0.49	1.81
ACO 1651	1006^{+135}_{-80}	965	965	2.14	0.07	0.94	0.46	1.02	0.16
ACO 1656 (Coma)	961^{+57}_{-55}	896	990	3.72	-0.18	0.96	0.10	2.22	1.11
ACO 1736a	382^{+37}_{-32}	366	366	2.00	0.20	0.90	0.27	1.27	0.51
ACO 1736b	903^{+72}_{-64}	873	873	2.13	-0.01	0.91	0.19	1.36	0.04
ACO 1750	875^{+163}_{-99}	774	774	4.25	-0.56	0.94	0.17	1.83	1.62
ACO 1795	788^{+114}_{-91}	786	786	3.01	0.27	1.12	0.78	0.02	0.72
ACO 1983	551^{+71}_{-47}	494	589	4.42	-1.07	0.91	0.00	2.45	3.65
ACO 1991	658^{+228}_{-114}	552	665	7.65	1.49	1.40	0.00	5.16	3.21
ACO 2052	750^{+244}_{-120}	575	575	4.79	1.31	1.31	0.00	2.47	3.54
ACO 2063	548^{+106}_{-70}	462	570	3.54	-0.60	1.37	0.17	0.71	1.56
ACO 2065	1247^{+249}_{-167}	1085	1085	3.13	-0.34	1.20	0.80	0.14	0.74
ACO 2079	739^{+177}_{-99}	651	651	4.04	0.77	1.38	0.25	1.17	1.70
ACO 2092	717^{+825}_{-230}	1614	530	4.24	-0.44	2.51	0.01	1.24	0.87
ACO 2147/2152	1413^{+154}_{-117}	1344	1344	2.04	0.45	0.93	0.02	1.28	1.18
ACO 2151 (Hercules)	826^{+74}_{-51}	757	825	3.14	0.37	0.93	0.30	0.28	1.51
ACO 2197	589^{+55}_{-69}	568	568	2.33	0.33	1.02	0.21	0.93	0.90
ACO 2199	818^{+71}_{-77}	797	797	2.57	0.05	1.19	0.58	0.70	0.18
ACO 2256	1348^{+89}_{-63}	1294	1294	2.06	0.19	0.88	0.01	1.83	0.72
ACO 2440	991^{+200}_{-117}	966	966	2.49	-0.70	0.86	0.09	0.56	1.48
ACO 2538	851^{+78}_{-60}	808	808	1.96	-0.32	0.92	0.03	1.45	0.87
ACO 2554	925^{+246}_{-100}	803	803	4.64	1.04	0.87	0.06	1.91	2.35
ACO 2589	621^{+310}_{-190}	799	799	4.33	0.04	2.20	0.02	1.66	0.09
ACO 2593	710^{+113}_{-68}	700	700	2.84	-0.37	1.00	0.66	0.21	0.94
ACO 2670	1030^{+59}_{-53}	954	1040	3.32	-0.51	1.07	0.00	0.94	2.95
ACO 2717	554^{+98}_{-56}	546	546	3.04	-0.08	1.11	0.97	0.04	0.21
ACO 2721	796^{+166}_{-113}	683	946	4.54	1.08	1.24	0.00	2.55	3.54
ACO 3126	1053^{+152}_{-104}	1029	1029	2.66	0.35	1.08	0.41	0.45	0.91
ACO 3128	845^{+129}_{-85}	843	843	2.91	0.70	0.91	0.05	0.13	1.93
ACO 3158	1043^{+164}_{-109}	1029	1029	2.79	0.59	1.01	0.39	0.27	1.46
ACO 3225	1098^{+119}_{-104}	1056	1056	2.16	-0.55	1.04	0.00	1.15	1.50
ACO 3266	1149^{+86}_{-74}	1106	1146	3.16	-0.14	1.18	0.78	0.38	0.67
ACO 3334	675^{+92}_{-72}	641	641	2.42	0.03	1.10	0.43	0.72	0.08
ACO 3360	849^{+151}_{-111}	779	779	4.65	0.56	1.25	0.10	2.18	1.44
ACO 3376	723^{+82}_{-61}	726	726	3.22	-0.16	1.09	1.00	0.38	0.53
ACO 3381	238^{+36}_{-35}	234	234	2.71	-0.24	1.11	0.79	0.34	0.55
ACO 3389	641^{+120}_{-54}	576	576	7.00	1.45	0.84	0.00	5.40	3.84
ACO 3391	1345^{+134}_{-96}	1244	1244	2.80	-0.05	0.93	0.72	0.34	0.17
ACO 3395	1093^{+88}_{-73}	1087	1087	2.88	0.53	1.17	0.00	0.30	2.63

TABLE 2—*Continued*

Name (1)	σ_{rob} (2)	σ_{YV} (3)	σ_{ZHG} (4)	K (5)	S (6)	STI (7)	$P(W)$ (8)	$\|K-3\|/\delta_K$ (9)	$\|S\|/\delta_S$ (10)
ACO 3526 (Centaurus)	923^{+40}_{-42}	874	874	2.98	-0.33	0.81	0.00	0.06	1.76
ACO 3532 (Klemola 22)	773^{+137}_{-102}	732	732	4.86	0.79	1.24	0.22	2.62	2.19
ACO 3558 (Shapley 8)	951^{+60}_{-52}	926	926	2.47	-0.03	0.88	0.56	1.17	0.13
ACO 3574	595^{+169}_{-84}	477	477	5.24	1.39	1.05	0.00	3.00	3.63
ACO 3667	1402^{+172}_{-152}	1380	1380	2.70	-0.22	1.14	0.66	0.44	0.63
ACO 3705	958^{+94}_{-76}	926	926	2.13	0.16	0.81	0.18	1.18	0.44
ACO 3716	954^{+141}_{-85}	783	783	4.98	1.12	0.87	0.00	3.66	4.10
ACO 4067	665^{+107}_{-74}	653	653	2.65	-0.10	1.16	0.96	0.42	0.23
ACO S301	506^{+223}_{-125}	453	658	7.79	1.50	1.87	0.00	5.67	3.46
ACO S373	336^{+27}_{-26}	324	324	2.25	0.12	0.95	0.33	1.19	0.39
ACO S463	619^{+48}_{-39}	603	603	2.40	-0.20	0.84	0.20	1.11	0.74
ACO S753	529^{+141}_{-88}	442	566	7.75	-1.38	1.33	0.00	6.03	3.44
ACO S805	470^{+66}_{-103}	484	484	3.22	-0.65	1.01	0.07	0.30	1.79
AWM 1	604^{+132}_{-62}	519	519	3.08	0.42	1.00	0.70	0.09	0.91
AWM 7	864^{+113}_{-81}	843	843	2.39	0.29	0.89	0.72	0.77	0.71
Colless 67	734^{+208}_{-148}	702	702	3.94	0.98	1.29	0.06	1.09	2.22
Dressler 0003-50	525^{+96}_{-61}	530	530	3.13	0.80	0.81	0.04	0.17	1.98
MKW 4	535^{+65}_{-59}	523	523	2.66	-0.17	1.04	0.44	0.48	0.47
Pegasus I	602^{+82}_{-74}	582	582	2.50	0.33	1.34	0.14	0.65	0.84
VIRGO	776^{+21}_{-21}	747	747	2.26	-0.09	0.98	0.00	3.09	0.77

EXPLANATION OF COLUMNS.—Col. (1): cluster name; Col. (2): robust velocity dispersion, σ_{rob}, with its associated bootstrap errors, at the 68% confidence level; Cols. (3) and (4): YV's estimate of velocity dispersion, σ_{YV}, and ZHG's estimate of velocity dispersion, σ_{ZHG}, respectively; Cols. (5), (6), (7), and (8): kurtosis, K; skewness, S; scaled tail index, STI; and probability associated to the W-test, $P(W)$, respectively; Cols. (9) and (10): the ratios $|(K-3)/\delta_K|$, and $|S/\delta_S|$. All quantities are computed inside 1.5 h_{100}^{-1} Mpc.

comparing the σ_{rob} distributions at 0.5, 1.0, and 1.5 h_{100}^{-1} Mpc, and we again found no significant difference.

We therefore conclude that the σ_{rob} distribution does not significantly depend on the sampling aperture.

In addition to the above analysis, we have compared the distributions of σ_{rob}, as evaluated in two contiguous regions, i.e., the circle of radius 0.5 h_{100}^{-1} Mpc and the annulus defined by the radii of 0.5 and 1.5 h_{100}^{-1} Mpc. We have considered only the 28 clusters with at least 20 galaxies inside each region, in order to have sufficiently good statistics. The two distributions are plotted in Figure 4. Although the KS, U, and T tests fail to detect a significant difference between the distributions, a systematic trend is apparent (and also detectable, using an appropriate statistical test, e.g., the sign test; see, e.g., Siegel 1956). The trend shows decreasing values of σ_{rob} with increasing clustercentric distance. Although this result should be regarded as preliminary, because of poor statistics, it agrees with previous findings (see, e.g., Kent & Gunn 1982; Kent & Sargent 1983; Sharples et al. 1988).

3.6. *Cluster Properties and Velocity Dispersion*

Danese et al. (1980) found that the mean velocity dispersions of their cluster sample increase with richness class, from $R = 0$ to $R = 2$, although their $R \geq 3$ cluster sample was considered too small for a meaningful statistical analysis. Bahcall (1981) showed the existence of a marginal correlation between velocity dispersions and Abell number counts, C, mostly due to the contribution of the poorest cluster.

In our cluster sample, σ_{rob} strongly correlates both with C(s.l. > 99.9%, Kendall correlation coefficient $r_K = 0.39$, on 69 clusters) and with R(s.l. > 99.9%, $r_K = 0.42$, on 75 clusters). The result holds at any limiting radius. The average value of σ_{rob} increases from 657 ± 45 km s^{-1}, for $R = 0$ (28 clusters), to 758 ± 40 km s^{-1} for $R = 1$ (25 clusters), to 989 ± 58 km s^{-1} for $R = 2$ (16 clusters). A mean value of 947 ± 51 km s^{-1} for $R \geq 3$, based on six objects only, hints at a possible flattening of this relation. A least-squares fit gives

$$\log \sigma_{rob} = 2.43(\pm 0.08) + 0.25(\pm 0.04) \log C \quad (1)$$

for the direct regression line, and

$$\log \sigma_{rob} = 1.8(\pm 0.2) + 0.6(\pm 0.1) \log C \quad (2)$$

for the bisecting line.

The presence of interlopers may seriously affect the evaluation of C(ACO); Bahcall (1977) suggested the use of the less contaminated richness parameter, N. We have therefore considered the relation between σ_{rob} and N. The s.l. of the correlation is >99.9%, and the correlation coefficient is $r_K = 0.50$ (on 22 clusters); i.e., N is more strongly correlated than C with σ_{rob}. The direct regression line is

$$\log \sigma_{rob} = 2.3(\pm 0.1) + 0.46(\pm 0.09) \log N \quad (3)$$

and the bisecting line is

$$\log \sigma_{rob} = 2.0(\pm 0.2) + 0.7(\pm 0.1) \log N \quad (4)$$

which has a very similar slope to equation (3). Figure 5 shows log σ_{rob} versus log C (*upper panel*) and versus log N (*lower panel*), with the bisecting regression lines.

We have computed both the direct and bisecting regression lines, since the former is used to predict the value of σ_{rob} from the richness, while the latter is used to estimate the underlying

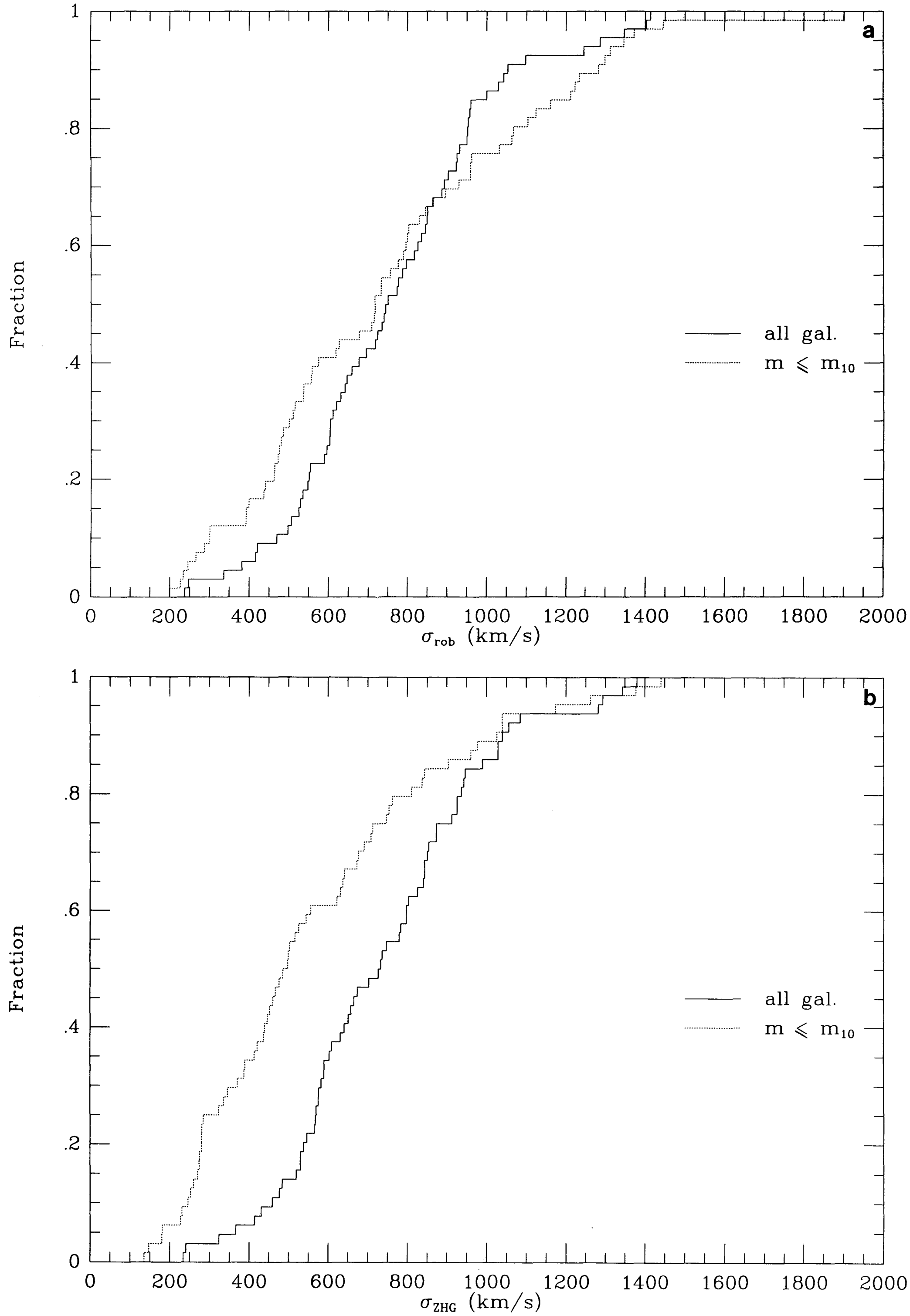

FIG. 3.—(*a*) Cumulative distributions of $\sigma_{\rm rob}$ for the total sample (*solid line*), and for the subsample of the galaxies brighter than m_{10} (*dotted line*). (*b*) As in (*a*), with $\sigma_{\rm ZHG}$ in lieu of $\sigma_{\rm rob}$. Only the two distributions of (*b*) are significantly different.

functional relation between the two quantities (see, e.g., Isobe et al. 1990).

Other optical properties of some importance are the morphological classifications by Bautz & Morgan (1970) and Rood & Sastry (1971; see also Struble & Rood 1987). ZHG did not find any difference between the average velocity dispersions of cD clusters and other types. In agreement with this result, we have not found any significant correlation between $\sigma_{\rm rob}$ and BM or RS types.

Moreover, we have also found that $\sigma_{\rm rob}$ is not significantly correlated either with the absolute magnitude of the first-ranked, m_1, or with the third-ranked, m_3.

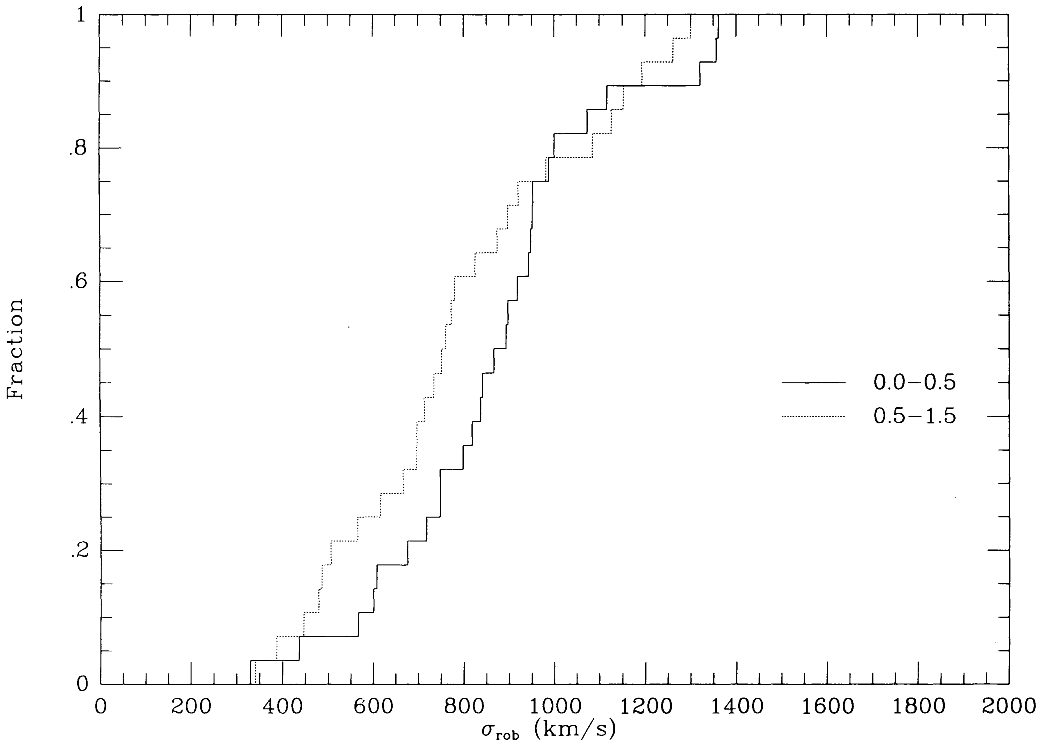

FIG. 4.—Cumulative distributions of $\sigma_{\rm rob}$ as evaluated in two contiguous regions, i.e., the circle of radius 0.5 h_{100}^{-1} Mpc (*solid line*, 0.0–0.5), and the annulus defined by the radii of 0.5 and 1.5 h_{100}^{-1} Mpc (*dotted line*, 0.5–1.5).

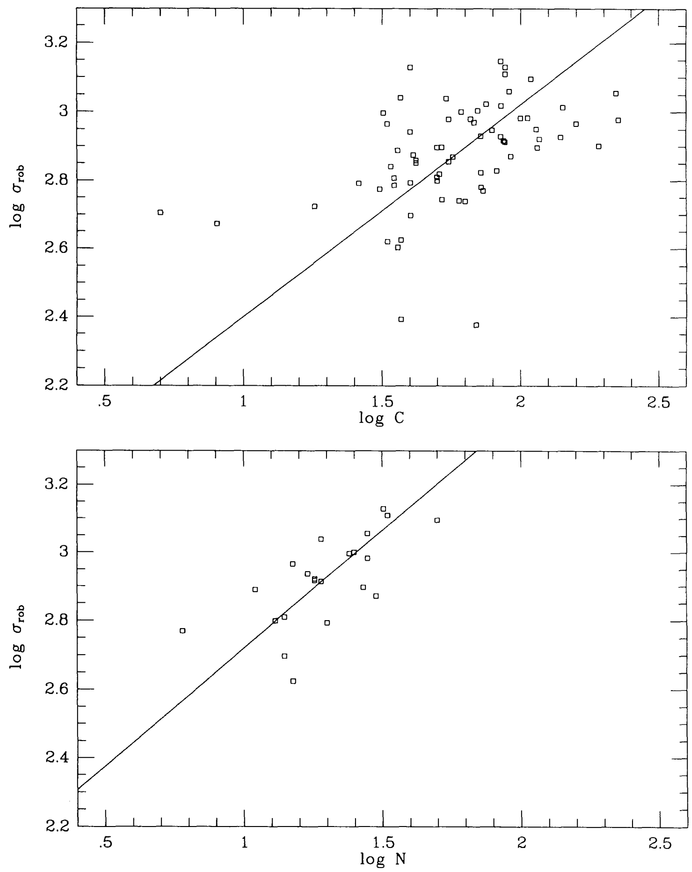

FIG. 5.—log $\sigma_{\rm rob}$ vs. log C (*top*) and vs. log N (*bottom*). The bisecting regression lines indicated have quite similar slopes.

3.7. *The Distribution Function of Cluster Velocity Dispersions*

The distribution function of cluster velocity dispersions can be used to test theories of large-scale structure formation. In order to do that, one has to be provided with a distribution function which is obtained from a complete cluster sample, e.g., that of ACOs. We recall that ACO's sample is nominally complete for $R \geq 1$, within $z \leq 0.2$, so we have neglected our $R = 0$ clusters. We have compared the R distribution for our sample of 47 $R \geq 1$ clusters, with the corresponding distribution for ACO's sample of $R \geq 1$ clusters (with redshift $\bar{z} \leq 0.15$, as obtained from m_{10}). Our sample being biased toward richer clusters, we have normalized our R distribution to that of ACOs. The normalization was accomplished by extracting 1000 values of $\sigma_{\rm rob}$ from our 47 clusters, according to ACO's R distribution (poor statistics forced us to consider clusters with $R \geq 3$ in the same class).

The resulting normalized distribution of $\sigma_{\rm rob}$ is not very different from the original one, as one can see in Figure 6, where we plot the cumulative distributions of $\sigma_{\rm rob}$, before and after normalization. The normalized distribution shows the cosmic distribution of the velocity dispersions of $R \geq 1$ clusters, on the hypothesis that our cluster sample is representative of the parent cluster population.

FWED calculated the distributions of velocity disperion in the standard CDM cosmogony for clusters with $R \geq 1$. We have compared the distribution of $\sigma_{\rm rob}$ for our cluster sample with FWED's theoretical predictions. Our normalized $\sigma_{\rm rob}$ distribution fits in well between the $b = 1.6$ and $b = 2$ distributions obtained by FWED from the simulations of clusters identified in three dimensions. Figure 7 shows our observational distribution in comparison with the theoretical distributions taken from FWED; the Poisson error bars are estimated by considering a total sample of 47 clusters.

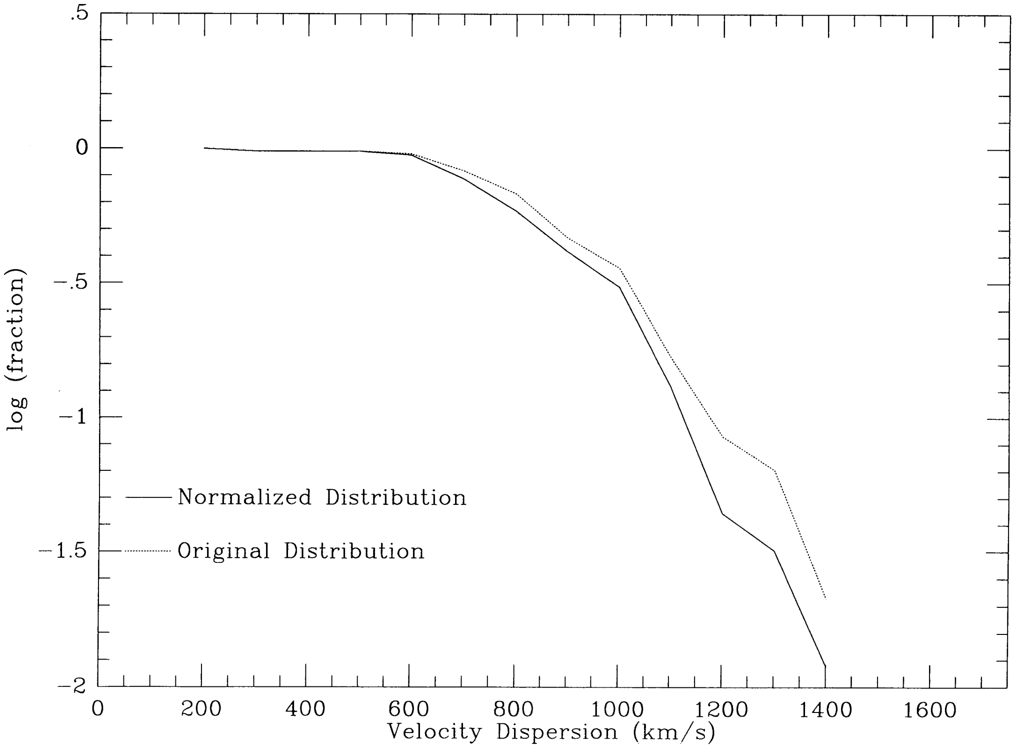

FIG. 6.—Our observational cumulative distribution of σ_{rob} for clusters with $R \geq 1$, before (*dotted line*) and after (*solid line*) normalization, according to ACO's distribution.

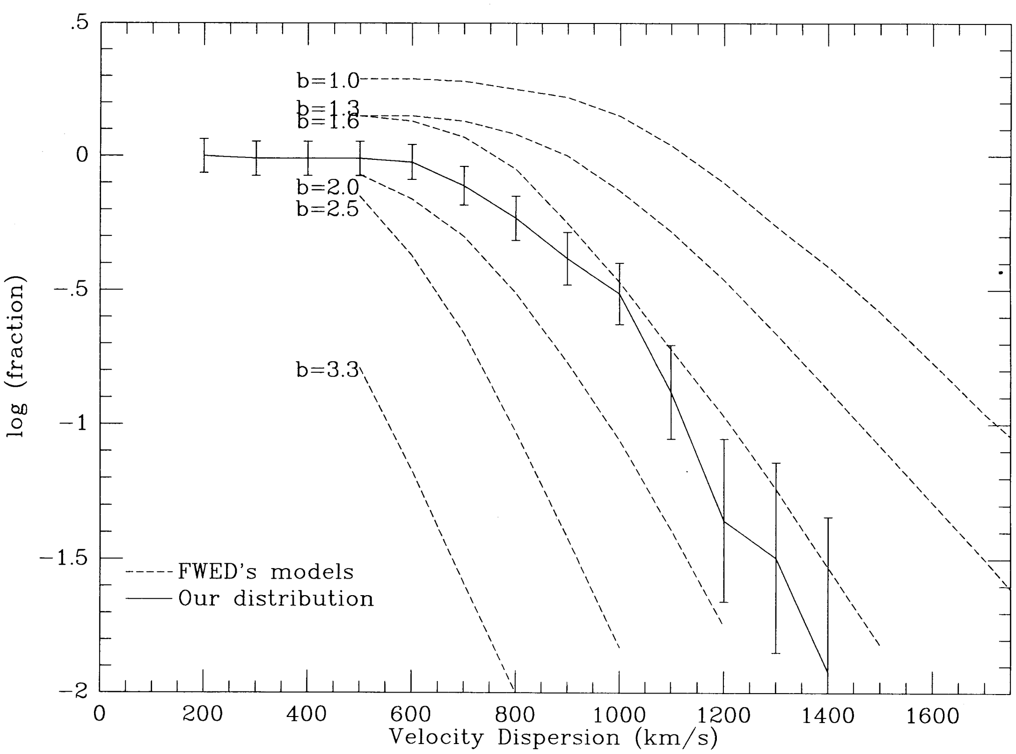

FIG. 7.—Cumulative (logarithmic) distributions of velocity dispersions: our observational normalized distribution (*solid line*), with Poisson error bars, compared with the theoretical distributions taken from FWED (*dashed lines*), labeled by the respective values of the biasing parameter, *b*.

4. DISCUSSION AND CONCLUSIONS

The analysis of the galaxy velocity distributions in our sample of 79 clusters has shown that the choice of the scale estimator is not fundamental, when more than 20 true cluster members are considered. We have compared the distributions of σ_{rob}, σ_{YV}, and σ_{ZHG} obtained at different limiting radii, and we have not found any significant differences.

A quasi-Gaussian distribution for the velocities of the cluster galaxies can well account for this result. In fact, the normality tests do not reject the hypothesis of Gaussianity for most of our cluster velocity distributions. This result is in agreement with previous findings (see, e.g., YV), and with theoretical expectation for a post–violent relaxation dynamical status (see, e.g., Sarazin 1986).

We have then examined the efficiency of the three scale estimators by artificially undersampling our cluster samples. Both σ_{ZHG} and, less significantly, σ_{YV}, underestimate the true velocity dispersions (as derived on the total sample), when only a few objects are considered (~ 10). The discrepancy is larger when the brightest objects are selected. This effect is probably induced by the poor efficiency of σ_{YV} and σ_{ZHG}, when working with small data sets (see also BFG). Moreover, when considering only the brightest galaxies, this effect is increased by the presence of luminosity segregation in the velocity space. The galaxies more luminous than the third-ranked move slower than the other galaxies: this segregation is an evidence of a more advanced dynamical status of virialization for these bright galaxies (see, e.g., Biviano et al. 1992 and references therein).

At variance with the other scale estimators, σ_{rob} behaves well by recovering the original estimate, also when the artificial undersampling is severe. We therefore support the suggestion of BFG to use σ_{rob} in scale estimates.

Nevertheless, we suggest that σ_{rob}, as computed on very few galaxies, should not be used in studies of individual clusters, but only of large sample distributions. In fact, the dispersion changes, on average, by $\sim \pm 200$ km s^{-1}, when a subsample of ~ 10 galaxies is selected from the original sample (see also the tails of the distributions plotted in Fig. 3).

The evaluation of the σ_{rob} distribution function may possibly be biased by a different limiting aperture for the observation of galaxies in different clusters (e.g., we notice that only 46 of our clusters have galaxies observed as far as 1.5 h_{100}^{-1} Mpc from the center). We have found that the distributions of σ_{rob} are not very sensitive to the limiting radius of the observational selection.

Evidence for subclustering has been claimed in many clusters (see, e.g., Baier 1978; Geller & Beers 1982; Bothun et al. 1983; Mazure et al. 1986; Dressler & Schectman 1988b; Fitchett & Webster 1987; Fitchett & Merritt 1988; Mellier et al. 1988; Rhee, van Haarlem, & Katgert 1991; Escalera & Mazure 1992; and references therein). The presence of substructures may influence the dynamics of the system and the evaluation of the velocity dispersion. In our sample there are 29 clusters which show significant evidence of subclustering, according to the test by Dressler & Schectman (1988b). We have not found any significant difference between the σ_{rob} distributions for all our clusters, and, respectively, for those clusters without evidence of a substructure. This result is consistent with the quasi-Gaussian distributions of velocities in most of our clusters. However, we have to recognize that the definition and the analysis of substructure is still being debated (see, e.g., West, Oemler, & Dekel 1988; West & Bothun 1990, and references therein), and it would require hundreds of redshifts for each cluster (see, e.g., Fitchett & Meritt 1988; Escalera & Mazure 1992). In view of these difficulties, we consider this result to be preliminary.

We have considered possible relations between σ_{rob} and other optical properties of our clusters. A significant correlation has been found to exist between σ_{rob} and richness, which is stronger when the Bahcall richness parameter, N, is used, instead of the Abell richness parameter, C. This result suggests that both N and C are mass tracers, but of different accuracy. The functional relations between log σ_{rob} and log N and log C, respectively, have notably the same slopes, within the errors. On the contrary, no significant correlation has been found between σ_{rob} and BM class or RS type, respectively.

Peebles et al. (1988) suggested a relation between b, the velocity dispersion and the richness, $b \propto$ richness/(dispersion)^2, on the hypothesis of an isothermal model for the cluster mass distribution. The b values, as derived from our σ_{rob}, correlate with the respective richness values, C, at a s.l. 99.99%; the bisecting regression line of log b versus log C has a slope of 1.1 ± 0.1. However, we do not find any correlation between b and N, which is consistent with a constant b for different richness.

The distribution function of velocity dispersions may be used to constrain theories of large-scale structure formation. Recently, DEFW, as well as the lastest *COBE* results on CBR (Bennett et al. 1992; Smoot et al. 1992), have called into question the whole CDM scenario. However, the CDM model is the only one that has been studied sufficiently in detail as to allow comparison with observational distribution functions of cluster velocity dispersions. So we have compared our distribution with the CDM model of FWED. Our distribution is in agreement with FWED's theoretical distribution for clusters identified in three dimensions, with $b \sim 1.6$–2.0.

The disagreement between our distribution and the observational distribution given by FWED possibly indicates a larger contamination by interlopers in the sample they used. On the contrary, our velocity dispersion distribution agrees with that of ZHGs, and both stress that a fair identification of cluster members does not lead to a large fraction of high-velocity dispersion clusters.

Detailed distribution function of observational cluster quantities can strongly constrain both cosmological scenarios and internal cluster dynamics. In the near future, we hope to enlarge our cluster sample and to provide the distribution functions of other fundamental cluster properties—sizes and masses in particular.

We wish to thank Alfonso Cavaliere, Bernard Jones, William Saslaw, Dennis Sciama, and Riccardo Valdarnini for their useful discussions. We also thank Tim Beers and Karl Gebhardt for kindly providing us with their ROSTAT software package, and George Rhee for the substructure analysis technique. We are indebted to the referee for the interesting comments. This work was partially supported by the Ministero per l'Università e per la Ricerca scientifica e tecnologica and by the Consiglio Nazionale delle Ricerche (CNR-GNA).

REFERENCES

Abell, G. O., Corwin, H. G., Jr., & Olowin, R. P. 1989, ApJS, 70, 1 (ACO)
Adams, M. T., Strom, K. M., & Strom, S. E. 1980, ApJ, 238, 445
Bahcall, N. A. 1977, ApJ, 217, L77
———. 1981, ApJ, 247, 787
Baier, F. W. 1978, Astron. Nach., 299, 311
Bautz, L. P., & Morgan, W. W. 1970, ApJ, 162, L149
Beers, T. C., Flynn, K., & Gebhardt, K. 1990, AJ, 100, 32 (BFG)
Beers, T. C., Forman, W., Huchra, J. P., Jones, C., & Gebhardt, K. 1991, AJ, 102, 1581
Beers, T. C., Geller, M. J., Huchra, J. P., Latham, D. W., & Davis, R. J. 1984, ApJ, 283, 33
Bell, M., & Whitmore, B. C. 1989, ApJS, 70, 139
Bennett, C. L., et al. 1992, preprint
Binggeli, B., Sandage, A., & Tammann, G. A. 1985, AJ, 90, 1681
Binggeli, B., Tammann, G. A., & Sandage, A. 1987, AJ, 94, 251
Biviano, A., Girardi, M., Giuricin, G., Mardirossian, F., & Mezzetti, M. 1992, ApJ, 396, 35
Bothun, G. D., Aaronson, M., Schommer, B., Mould, J., Huchra, J., & Sullivan, W. T., III 1985, ApJS, 57, 423
Bothun, G. D., Geller, M. J., Beers, T. C., & Huchra, J. P. 1983, ApJ, 268, 47
Burstein, D., & Heiles, C. 1982 AJ, 87, 1165
Butcher, H. R., & Oemler, A., Jr. 1985, ApJS, 57, 665
Cavaliere, A., Colafrancesco, S., & Scaramella, R. 1991, ApJ, 380, 15
Chapman, G. N. F., Geller, M. J., & Huchra, J. P. 1987, AJ, 94, 571
———. 1988, AJ, 95, 999
Chincarini, G., & Rood, H. J. 1976, PASP, 88, 388
———. 1977, ApJ, 214, 351
Chincarini, G., Tarenghi, M., & Bettis, C. 1981, A&A, 96, 106
Colless, M. 1989, MNRAS, 237, 799
Colless, M., & Hewett, P. 1987, MNRAS, 224, 453
Cristiani, S., de Souza, R., D'Odorico, S., Lund, G., & Quintana, H. 1987, A&A, 179, 108
Danese, C., De Zotti, G., & di Tullio, G. 1980, A&A, 82, 322
Davis, M., Efstathiou, G., Frenk, C. S., & White, S. D. M. 1992, Nature 356, 489 (DEFW)
de Vaucouleurs, G. 1977, in The Evolution of Galaxies & Stellar Population, ed. B. M. Tinsley & R. B. Larson (New Haven: Yale Univ. Obs.)
Dickens, R. J., Currie, M. J., & Lucey, J. R. 1986, MNRAS, 220, 679
Dickens, R. J., & Moss, C. 1976, MNRAS, 174, 47
Dressler, A. 1980, ApJS, 42, 565
Dressler, A., & Shectman, S. A. 1988a, AJ, 95, 284
———. 1988b, AJ, 95, 985
Efron, B., & Tibshirani, R. 1986, Statistical Science, 1, 54
Escalera, E., & Mazure, A. 1992, ApJ, 388, 23
Evrard, A. E. 1989, ApJ, 341, L71
Fabricant, D. G., Kent, S. M., & Kurtz, M. J. 1989, ApJ, 336, 77
Fanti, C., et al. 1982, A&A, 105, 200
Fitchett, M. J., & Merritt, D. 1988, ApJ, 335, 18
Fitchett, M. J., & Webster, R. L. 1987, ApJ, 317, 653
Frenk, C. S., White, S. D. M., Efstathiou, G., & Davis, M. 1990, ApJ, 351, 10 (FWED)
Gavazzi G. 1987, ApJ, 320, 96
Gebhardt, K., & Beers, T. C. 1991, ApJ, 383, 72
Geller, M. J., & Beers, T. C. 1982, PASP, 94, 421
Geller, M. J., Beers, T. C., Bothun, G. D., & Huchra, J. P. 1984, AJ, 89, 319
Giovanelli, R., Haynes, M. P., & Chincarini, G. L. 1982, ApJ, 262, 442
Gregory, S. A., & Thompson, L. A. 1984, ApJ, 286, 422
Gregory, S. A., Thompson, L. A., & Tifft, W. G. 1978, ApJ, 222, 784
———. 1981, ApJ, 243, 411
Guest, P. G. 1961, Numerical Methods of Curve Fitting (Cambridge: Cambridge Univ. Press)
Henry, J. P., & Arnaud, K. A. 1991, ApJ, 372, 410
Hill, J. M., Hintzen, P., Oegerle, W. R., Romanishin, W., Lesser, M. P., Eisenhamer, J. D., & Batuski, D. J. 1988, ApJ, 332, L23
Hintzen, P., Hill, J. M., Lindley, D., Scott, J. S., & Angel, J. R. P. 1982, AJ, 87, 1656
Hoel, P. G. 1971, Introduction to Mathematical Statistics (New York: J. Wiley & Sons)
Inagaki, S., Itoh, M., & Saslaw W. C. 1992, ApJ, 386, 9
Isobe, T., Feigelson, E. D., Akritas, M. G., & Babu, G. J. 1990, ApJ, 364, 104
Kendall, M., & Stuart, A. 1977, The Advanced Theory of Statistics (London: Griffin)
Kent, S. M., & Gunn, J. E. 1982, AJ, 87, 945
Kent, S. M., & Sargent, W. L. W. 1983, AJ, 88, 697
Kirshner, R. P., Oemler, A., Jr., & Schechter, P. L. 1978, AJ, 83, 1549
Lauberts, A., & Valenttijn, E. A. 1989, The Surface Photometry Catalogue of the ESO-Uppsala Galaxies (Garching bei München: European Southern Observatory)
Ledermann, W. 1982, Handbook of Applicable Mathematics, 6 (New York: Wiley)
Lilje, P. B. 1992, ApJ, 386, L33
Lilje, P. B., & Lahav, O. 1991, ApJ, 374, 29
Lucey, J. R., Dickens, R. J., Mitchell, R. J., & Dawe, J. A. 1983, MNRAS, 203, 545
Malumuth, E. M., & Kriss, G. A. 1986, ApJ, 308, 10
Mazure, A., Gerbal, D., Proust, D., & Capelato, H. V. 1986, A&A, 157, 159
Mellier, Y., Mathez, G., Mazure, A., Chauvineau, B., & Proust, D. 1988, A&A, 199, 67
Metcalfe, N., Godwin, J. G., & Spenser, S. D. 1987, MNRAS, 225, 581
Moss, C., & Dickens, R. J. 1977, MNRAS, 178, 701
Newberry, M. V., Kirshner, R. P., & Boronson, T. A. 1988, ApJ, 335, 629
Nilson, P. 1973, Uppsala General Catalogue of Galaxies (Stockholm: Almquist and Wiksell)
Oemler, A., Jr. 1974, ApJ, 194, 1
Ostriker, E. C., Huchra, J. P., Geller, M. J., & Kurtz, M. J., 1988, AJ, 96, 177
Peebles, P. J. E., Daly, R. A., & Juszkiewicz, R. 1989, ApJ, 347, 563
Phillips, S., Fong, R., & Shanks, T. 1981, MNRAS, 194, 49
Postman, M., Geller, M. J., & Huchra, J. P. 1988, AJ, 95, 267
Postman, M., Huchra, J. P., & Geller, M. J. 1986, AJ, 92, 1238
Press, W. H., & Schechter, P. 1974, ApJ, 187, 425
Proust, D., Mazure, A., Sodré, L., Capelato, H. V., & Lund, G. 1988, A&AS, 72, 415
Proust, D., Quintana, H., Mazure, A., de Souza, R., Escalera, E., Sodré, L., Jr., & Capelato, H. V. 1992, A&A, 258, 243
Quintana, H., Melnick, J., Infante, L., & Thomas, B. 1985, AJ, 90, 410
Rhee, G., van Haarlem, M., & Katgert, P. 1991, A&A, 246, 301
Richter, O. G. 1987, A&AS, 67, 237
———. 1989, A&AS, 77, 237
Richter, O. G., & Huchtmeier, W. K. 1982, A&A, 109, 155
Rood, H. J., & Sastry, G. N. 1971, PASP, 83, 313
Sandage, A. 1973, ApJ, 183, 711
Sarazin, C. L. 1986, Rev. Mod. Phys., 58, 1
Schneider, D. P., Gunn, J. E., & Hoessel, J. G. 1983, ApJ, 264, 337
Schweizer, F. 1976, ApJ, 31, 313
Scott, D. Rees, M. J., & Sciama, D. W. 1991, A&A, 250, 295
Shanks, T., Stevenson, P. R. F., Fong, R., & MacGillivray, H. T. 1984, MNRAS, 206, 767
Shapiro, S. S., & Wilk, M. B. 1965, Biometrika, 52, 591
Sharples, R. M., Ellis, R. S., & Gray, P. M. 1988, MNRAS, 231, 479
Siegel, S. 1956, Nonparametric Statistics for the Behavioral Sciences (New York: McGraw-Hill), 68
Smoot, G. F., et al. 1992, ApJ, 396, L1
Struble, M. F., & Rood, H. S. 1987, ApJS, 63, 555
———. 1991, ApJ, 374, 395
Tarenghi, M., Tifft, W. G., Chincarini, G., Rood, H. J., & Thompson, L. A. 1979, ApJ, 234, 793
Teague, P. F., Carter, D., & Gray, P. M. 1990, ApJS, 72, 715
Tifft, W. G. 1974, ApJ, 188, 221
———. 1978, ApJ, 222, 54
Thuan, T. X., & Gunn, J. E. 1976, PASP, 88, 543
Trimble, V. 1987, ARA&A, 25, 425
West, M. J., & Bothun, G. D. 1990, ApJ, 350, 36
West, M. J., Oemler, A., & Dekel, A. 1988, ApJ, 327, 1
Willmer, C. N. A., Forcardi, P., Chan, R., Pellegrini, P. S., & Nicolaci Da Costa, L. 1991, AJ, 101, 57
Yahil, A., & Vidal, N. 1977, ApJ, 214, 347 (YV)
Zabludoff, A. I., Huchra, J. P., & Geller, M. J. 1990, ApJS, 74, 1 (ZHG)
Zwicky, F., Herzog, E., Wild, P., Karpowicz, M., & Kowal, C. 1961–1968, Catalog of Galaxies and of Clusters of Galaxies 1–6 (Pasadena: Caltech)